PRELIMINARY GEOLOGIC MAP OF MOUNT PAGAN VOLCANO, PAGAN ISLAND, COMMONWEALTH OF THE NORTHERN MARIANA ISLANDS

By Frank A. Trusdell[1], Richard B. Moore[2], and Maurice K. Sako[1]
[1]Hawaiian Volcano Observatory, Hawaii National Park, Hawaii 96718; *trusdell@usgs.gov*
[2]US Geological Survey, Tucson, Arizona 95704

Prepared in cooperation with the Emergency Management Office, Commonwealth of the Northern Mariana Islands

Open-File Report
2006-1386

2006
U.S. Department of the Interior
U.S. Geological Survey

INTRODUCTION

GEOLOGIC SETTING

Pagan Island is the subaerial portion of two adjoining Quaternary stratovolcanoes near the middle of the active Mariana Arc, north of Saipan (fig. 1). Pagan and the other volcanic islands that constitute part of the Arc form the northern half of the East Mariana Ridge, which extends about 2-4 km above the ocean floor. The > 6-km-deep Mariana Trench adjoins the East Mariana Ridge on the east, and the Mariana Trough, partly filled with young lava flows and volcaniclastic sediment, lies on the west of the Northern Mariana Islands (East Mariana Ridge; Tanakadate, 1940; Hess, 1948; Karig, 1971; Karig and others, 1978; Banks and others, 1984). The submarine West Mariana Ridge, Tertiary in age (Kroenke and others, 1981), bounds the western side of the Mariana Trough. The Mariana Trench and Northern Mariana Islands (East Mariana Ridge) overlie an active subduction zone where the Pacific Plate, moving northwest at about 10.3 cm/year, is passing beneath the Philippine Plate, moving west-northwest at 6.8 cm/year (Simkin and others, 1989). Beneath the Northern Mariana Islands, earthquake hypocenters at depths of 50-250 km identify the location of the west-dipping subduction zone, which farther west becomes nearly vertical and extends to 700 km depth (Katsumata and Sykes, 1969). During the past century, more than 40 earthquakes of magnitude *6.5-8.1* have shaken the Mariana Trench (National Earthquake Information Center, unpub. data).

The Mariana Islands form two sub-parallel, concentric, concave-west arcs (fig. 1). The southern islands comprise the outer arc and extend north from Guam to Farallon de Medinilla. They consist of Eocene to Miocene volcanic rocks and uplifted Tertiary and Quaternary limestone (Gilbert Corwin, unpub. data, 1971). The nine northern islands extend from Anatahan to Farallon de Pajaros and form part of the inner arc. The active inner arc extends south from Anatahan, where volcanoes, some of which are active, form seamounts west of the older outer arc (fig. 1; Karig, 1971; Stern and Bibee, 1984). Other volcanic seamounts of the active arc surmount the East Mariana Ridge in the vicinity of Anatahan and Sarigan and north and south of Farallon de Pajaros (Karig, 1971). Six volcanoes (Farallon de Pajaros, Asuncion, Agrigan, Mount Pagan, Guguan, and Anatahan) in the northern islands have erupted during the past century (Tanakadate, 1940; Trusdell and others, 2005), and Ruby Seamount erupted in 1996 (R.Y. Koyanagi, unpub. data).

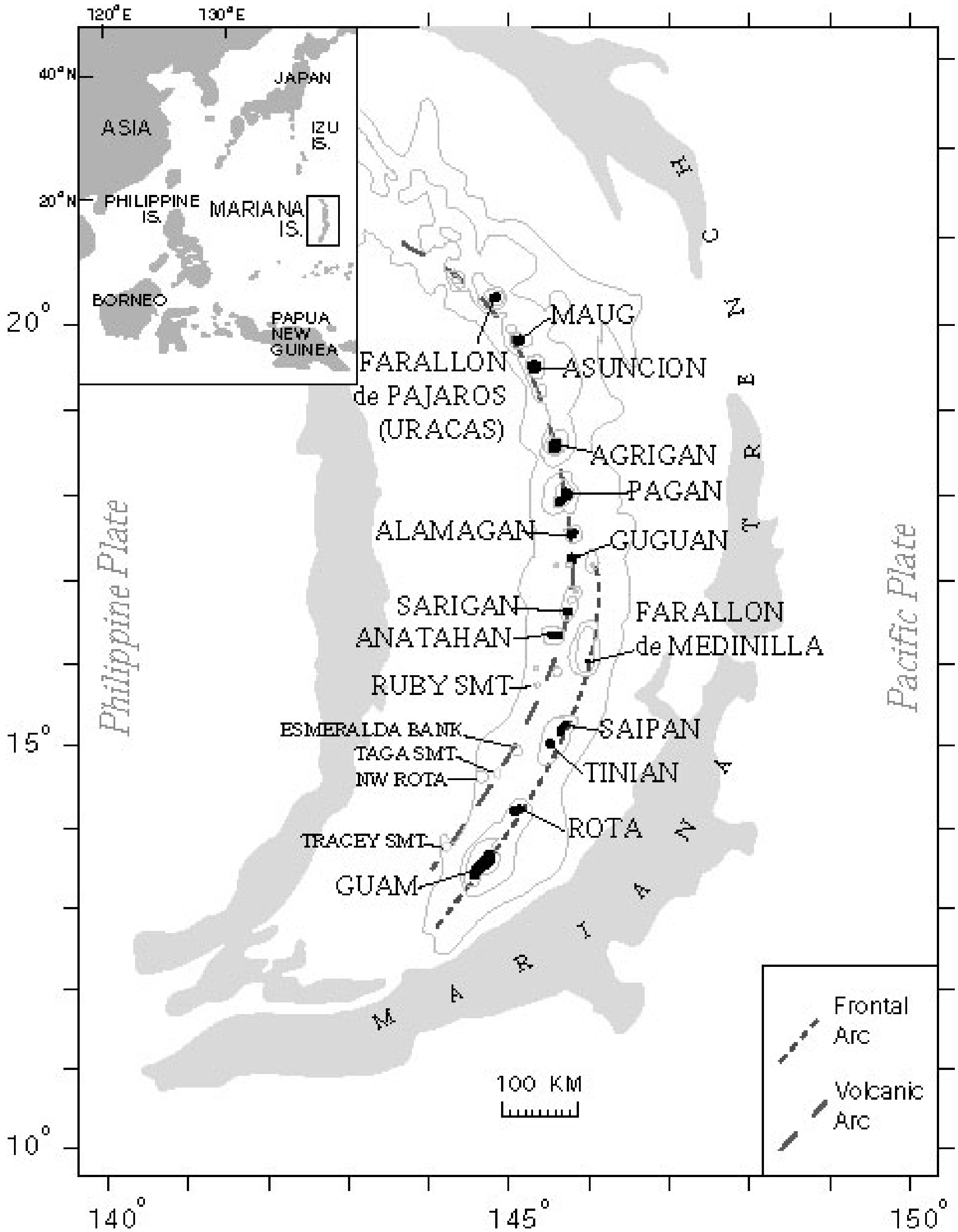

Figure. 1. Regional map of the Mariana Islands and outline of the adjacent Mariana Trench. The Commonwealth of the Northern Mariana Islands extends from Rota in the south to Uracas in the north.

PREVIOUS INVESTIGATIONS

Despite centuries of settlement, few detailed studies have been made of the geology and historic eruptive activity of Mount Pagan. A few eruptions were reported as early as the 1600s; a large eruption was reported in 1872–73, and relatively minor activity was noted during the 1920s. After the United States annexed the Marianas in the aftermath of World War II, Corwin and others (1957) assessed the geology of Pagan Island and constructed a geologic map distinguishing different rock types, like tuff, clinker ‘a‘ā, pāhoehoe, and cinders, partly on the basis of their suitability as construction materials.

The large Plinian eruption of Mount Pagan on May 15, 1981, resulted in the evacuation of Pagan residents (Banks and others, 1984). Intermittent ejection of mainly phreatic ash and other products continued for another 15 years. The U.S. Geological Survey operated two seismometers on the island, chiefly during the 1990s and in 2001, but, at present, there is no continuous monitoring.

CLIMATE

The climate of Mount Pagan is dominated by northeast trade winds, which bring frequent heavy showers during much of the year, except in late spring and early summer. Typhoons and tropical storms are common in the Northern Mariana Islands, especially from August to December. Average annual rainfall on Pagan is about 178-203 cm (70-80 inches; Corwin and others, 1957).

STRUCTURE AND MORPHOLOGY

Rocks erupted by Mount Pagan cover an area of about 8 km in a north-south direction by 6 km west-east. A 5.5-km-diameter (fig. 2), roughly circular caldera, with a prominent southern wall and more subdued, partly buried northern and eastern scarps includes more than half of the subaerial part of Mount Pagan. Preliminary calculations of the volume of the volcanic edifice that occupied the remnant caldera are ~4.7 to 5.8 km^3. This implies that the caldera-forming eruption was large and, at least, a VEI 5 (Newhall and Self, 1982; Mt St. Helens in 1980 was a VEI 5). Mount Pagan itself rises to an elevation of 570 m near the center of the caldera. On the western flank of Mount Pagan is a roughly 2 x 2-km depression with a lake in its floor (fig. 2). The deposits surrounding the depression are characteristic of phreatomagmatic eruptions. We interpret this feature as a maar.

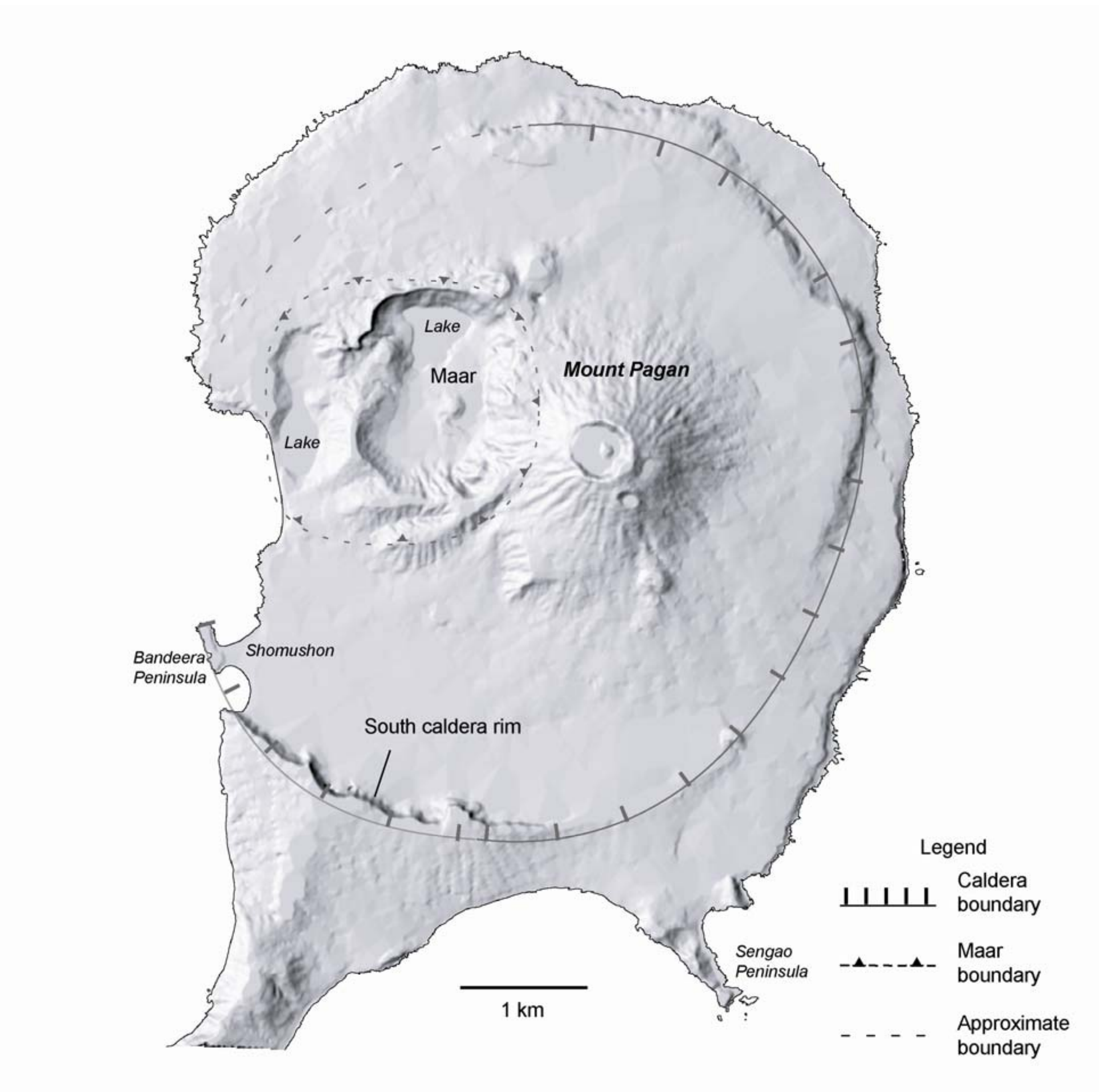

Figure 2. North Pagan map showing the boundaries of the caldera and maar.

We have obtained about a dozen radiocarbon ages from charcoal collected beneath lava flows and within pyroclastic deposits. An age of 10,780 ± 250 years B.P. for a lava flow near the base of the southwestern caldera wall suggests that most of the stratigraphic succession above it, including the presumed caldera-forming unit, is Holocene in age. Most of our new age determinations are only a few hundred years old, suggesting that Mount Pagan has erupted frequently and grown rapidly since caldera formation, probably less than 1,000 years ago. Hence, it must be regarded as a potentially dangerous volcano.

Erosion has not been as prominent on Mount Pagan as it has been on some other islands in the chain, perhaps due to the many lava flows and a lower abundance of loose pyroclastic materials. However, localized erosion has been prominent in large drainages that head on the western upper flank of Mount Pagan and flow southwestward into Shomushon village. Unfortunately, the village has been mostly destroyed by flooding and debris flows after the 1981 eruption.

RADIOCARBON DATA

This report includes 10 radiocarbon ages from 3 eruptive units (table 1). Most of the ages are Accelerator Mass Spectrometer ages generated in the U.S. Geological Survey's laboratory in Reston, Virginia. In addition, two ages were obtained from other laboratories. All ages are reported in radiocarbon years before present (yr B.P., before the calendar year datum of A.D. 1950). The variance is reported as one standard deviation, in years.

Carbonized roots, twigs, or vegetative litter formed most samples; rarely, unaltered wood was used. Each age was calibrated to calendar years using CALIB 4.0 Radiocarbon Calibration Program (Stuiver and others, 1998). The calibrated ages are for two standard deviations. The data in column Table 1 labeled "Age range" encompasses the entire age range of calendar ages possible for a given radiocarbon age. Symbols indicating quality show usefulness of age in stratigraphic interpretations: +, age thought meaningful; 0, age probably meaningful but accuracy may be far poorer than indicated by the reported precision; -, age meaningless (owing to large analytical error) or incorrect (on the basis of our knowledge obtained by all ages and regional stratigraphic relationships). Meaningless ages are not reported in Table 1.

Table 1. Radiocarbon ages of samples from North Pagan, CNMI. [All ages are reported in radiocarbon years before present (yr B.P., before the calendar year datum of A.D. 1950). The variance is reported as one standard deviation in years. Materials dated include charcoal, roots, twigs, vegetative litter, or unaltered wood

Table 1. Radiocarbon ages of samples from North Pagan, CNMI

[All ages are reported in radiocarbon years before present (yr B.P., before the calendar year datum of A.D. 1950). Materials dated include charcoal, roots, twigs, vegetative litter, or unaltered wood (rarely).]

Unit Label	Age[1] Group	Quality[2]	Field No.	Lab No.	Age[3] yr B.P.	S.D.[3] yr.	Age Range[4]	Location	Latitude (degree[5])	Longitude (degree[5])	Elev. (ft)
Qbp5	1	+	TM-01-05c	WW 3687	235	35	1524 to 1952	N Pagan N Coast on beach	18.16574	145.78893	10
Qbp5	1	+	TM-01-11	WW 3692	235	35	1524 to 1952	Inland lake and coast	18.13737	145.77080	120
Qbp5	0	-	TM-01-09c	WW 3690	50	35	1693 to 1955	West of inner lake	18.13724	145.77408	120
Qbp5	1	+	TM-01-10	WW 3691	110	35	1680 to 1954	West of inner lake	18.13723	145.77396	120
Qbp5	1	+	TM-01-14	WW 3644	105	35	1681 to 1954	SW end of outer lake	18.13922	145.76249	10
Qbp5	1	+	MM-92-33		600	89	1229 to 1454	W coast Sof Laguna Sanhiyon	18.13334	145.76067	5
Qaf29	11	+			10780	200	11158 to 10194	Crater wall under massive flow	18.12180	145.75816	30
Qbf3	1	+	PAG-94-1	WW 547	170	50	1652 to 1953	S Flank Mt. Pagan	18.12870	145.79050	130
Qbp5	0	+	PAG-94-2	WW 548	110	60	1669 to 1954	Shomushon bay	18.13030	145.76560	8
Qbp5	1	+	PAG-94-3	WW 549	250	60	1468 to 1952	Mt. Pagan WSW coast	18.13290	145.76560	15

[1]Age group:

0	flows formed A.D. 1843 to 1984	7	6,000-7,000 yr B.P.
1	flows 150-1,000 radiocarbon yr B.P.	8	7,000-8,000 yr B.P.
2	flows 1,000-2,000 yr B.P.	9	8,000-9,000 yr B.P.
3	flows 2,000-3,000 yr B.P.	10	9,000-10,000 yr B.P.
4	flows 3,000-4,000 yr B.P.	11	10,000-15,000 yr B.P.
5	4,000-5,000 yr B.P.	12	15,000-20,000 yr B.P.
6	5,000-6,000 yr B.P.	13	> 20,000 yr B.P.

[2]Quality: + = age thought meaningful; 0 = age probably meaningful but accuracy may be poorer than indicated by the reported precision. Meaningless '(large analytical error) or incorrect (using all age data and regional stratigraphic relationships) ages are not reported here; see Appendix A.

3Calibrated ages are for two standard deviations.

[4]Each age was calibrated to calendar years using CALIB 4.0 Radiocarbon Calibration Program (Stuiver and others, 1998); calibrated ages are for two standard deviations. Entire age range of calendar ages possible for a given sample. Unspecified ages are A.D.; BC and - (negative) = B.C.

[5]Datum, WGS84; projection, Geographic (dd)

MAP UNIT SYMBOLS

All units and surficial deposits of Mount Pagan are Quaternary (Q) in age. Compositions (IUGS system; LeBas and others, 1986), where known, are either basalt (b) or basaltic andesite (a) or a combination of the two (ba). Rocks crop out in cinder or spatter cones (c), lava flows (f), or consolidated or unconsolidated pyroclastic deposits (p).

All flows are numbered and based on stratigraphy. Undated flows are correlated to dated flows using superposition. Units that are stacked show direct superposition relations (young over old flows). Question mark indicates that the base of the flow is concealed. For units that are not in contact we use surface exposure; color change due to solar radiation; extend of weathering; tree height, size, and girth; diversity of native plant species; soil and ash accumulation to assign stratigraphic order.

DESCRIPTION OF MAP UNITS

UNITS OF HISTORIC AGE (A.D. 1600 and younger)

Qbc1 Qbf1 Qbp1 1981

Spatter and cinder deposits and ‘a‘ā and minor pāhoehoe flows erupted mainly in 1981 (Banks and others, 1984) from Mount Pagan. Intermittent light ejection of chiefly phreatic ash continued until 1996, with maximum post-1981 accumulation estimated at as much as 1-2 m on the source cone. Volume of erupted basalt is estimated to be > 200 x 10^6 m^3. Unit Qbc1-1981 includes a large mass of flow-rafted spatter on the north lower flank of Mount Pagan. Qbc1-1981 in the main summit crater of Mount Pagan also includes unmapped pāhoehoe and ‘a‘ā flows. One early estimate of commercial grade pozzolan of unit Qbp1 is about 65 million metric tons (http://www.azmarinternational.com/product.htm). Banks and others (1984) estimated the volume of pozzolan to be 28 x 10^6 m^3 Using isopachs from Banks and others (1984) and a revised estimate of basalt density; we estimate about 32 million metric tons. Taking into account the lower density of vesicular basalt and tephra, we consider this as a minimum (see appendix B for our revised estimate of Banks and others, volume of pozzolan; Appendix C is a Chemical

Assay of the 1981 tephra). Basalt has 1-7 percent plagioclase, 1-7 percent clinopyroxene, and less than 1 percent olivine phenocrysts (Banks and others, 1984).

Qbp2 Qbf2 A.D. 1925

Cinders, ‘a‘ā, and pāhoehoe flows erupted in 1925 (Newhall and Dzurisin, 1988; Simkin and Siebert, 1994). Source vent was the summit of Mount Pagan, and prior to the 1981, eruption a small cone (marked 502 m on the military-created topographic base) that formed during the 1925 eruption lay on the floor of the main crater of Mount Pagan (Corwin and others, 1957). Other small eruptions, mainly of cinders and ash but not lava flows, were reported mainly during the 1920’s (Simkin and Siebert, 1994) and the deposits of these eruptions are included in map unit Qbp2. Unit is mostly buried by the products of the 1981-1996 eruptions. Basalt has 10-15 percent plagioclase and less than 1 percent olivine phenocrysts.

Qbf3 A.D. 1872–73

Extensive ‘a‘ā and pāhoehoe flows possibly erupted in A.D. 1872-73 (Newhall and Dzurisin, 1988; Simkin and Siebert, 1994). Source vent was Mount Pagan, but all vent materials erupted at this time appear to be buried by the products of later eruptions, particularly those of 1981. Tentative age is assigned on the basis of published reports (summarized in Newhall and Dzurisin, 1988), stratigraphic relationships, and the presence of fresh, uneroded, and relatively pristine morphology of delicate primary features on flow surfaces. Basalt has 1-3 percent plagioclase and less than 1 percent olivine phenocrysts.

UNITS OF HOLOCENE AGE

Qbc4 Qbf4

Cinder cone and pāhoehoe flow on floor of larger eastern maar crater about 1 km west-northwest of summit crater of Mount Pagan. Possibly, this unit represents the latest episode in eruption of maar Qbp5. Basalt has 15-20 percent plagioclase and 2-3 percent olivine phenocrysts.

Qbp5

Extensive maar and its associated pyroclastic-flow and -surge deposits on the western flank of Mount Pagan. Several radiocarbon ages range from about 600 to 50 years B.P., suggesting that eruption occurred intermittently over a long period of time, perhaps triggered by ascent of several different batches of magma into a large hydrothermal and hydrologic system near sea level within the volcano. The radiocarbon ages span a time period when Pagan likely was populated, but most of the western side of the volcano must have been repeatedly devastated, making habitation difficult. The western outer lake, Laguna Sanhiyon, is salty like the adjacent ocean (fish live in it) and the eastern inner lake, Laguna Sanhalom, is less so, probably because of dilution by rainfall. Hot springs occur adjacent to the inner lake. Laguna Sanhiyon occupies the smaller western maar crater. It may be slightly older than the eastern larger crater. 600 ± 89 year old charcoal was found in the basal tuff in this area. At the other end of the age range, unit Qbc4, Qbf4 may be of historical age. Unit is locally mantled by as much as 1 m of 1981 cinders (unit Qbpl-1981). Not shown where underlying units can be recognized. Chemical compositions of aphyric juvenile pumice from the coarser pyroclastic-flow deposits are basaltic andesite. Age ranges from 50 to 600 yr B.P.

Qbc6 Qbf6

Pair of cones on the north flank of Mount Pagan adjacent to the large maar on its northeast side, and an extensive ‘a‘ā and pāhoehoe flows of Marasu. Stipple pattern on topographic base map portrays the pre-1981 mantle of ash and tuff, mainly a thin unmapped part of unit Qbp5 that covers much of unit Qbf6. Units Qbc6, Qbf6 also are mostly buried by 1981 cinders. Basalt has 15-20 percent plagioclase and less than 1 percent olivine phenocrysts.

Qbc7 Qbf7

Spatter deposits on the southeast flank of Mount Pagan and pāhoehoe and ʻaʻā flows at the old caldera scarp. Basalt has 12-15% percent plagioclase and 1-2 percent olivine phenocrysts. Microgabbroic clusters 1 cm in diameter are common.

Qbc8

Small spatter cone on lower south flank of Mount Pagan. Overlain by Qbf3. Basalt has 10-15 percent plagioclase and about 1 percent olivine phenocrysts.

Qbc9

Small spatter cone on middle east flank of Mount Pagan. Basalt has 7-10 percent plagioclase and about 1 percent olivine phenocrysts in a variably glassy groundmass.

Qbc10 Qbf10

Spatter cone, pāhoehoe and ʻaʻā flows on the lower southeast flank of Mount Pagan, just inside the southeast caldera wall. Overlain by Qbf7. Basalt has 10-20 percent plagioclase, 1-2 percent olivine, and less than 1 percent pyroxene phenocrysts.

Qbf11

ʻAʻā flow on the lower southwest flank of Mount Pagan, surrounding cone Qbc12. Source vent is not known but likely was near the summit of Mount Pagan. Flow has 20-25 percent plagioclase and <1 percent olivine phenocrysts.

Qbc12

Spatter cone on the lower southwest flank of Mount Pagan, surrounded by younger lava flows and is located about 1 km east-northeast of Shomushon. Basalt has 10-15 percent plagioclase and less than 1 percent olivine phenocrysts.

Qbc13

Eroded spatter cone at coastal beach about 1 km south of Shomushon. Basalt has 3-5 percent plagioclase phenocrysts.

Qbc14

Large Surtseyan tuff cone at coast on east side of peninsula linking Mount Pagan and South Pagan, about 1 km south of the south caldera wall of Mount Pagan. Juvenile basalt bombs have 10-15 percent plagioclase and 5-7 percent olivine phenocrysts.

Qbap15

Massive tuff breccia with associated pyroclastic-flow and surge deposits, accretionary lapilli, and unconsolidated tuff and ash. Unit is about 50 m thick on the south and east caldera walls and more than 40 m thick on the north caldera wall and sea cliff. Eruption of this unit, which typically caps the precaldera stratigraphic sequence on the north, east, and south caldera walls, probably led to collapse of the 5.5-km-diameter caldera. Volume of the unit is difficult to estimate because most of it was deposited in the sea, but it is probably several cubic kilometers. Unit overlies a basaltic andesite flow on the north caldera wall and adjoining sea cliff that has a radiocarbon age of 235 ± 35 years B.P., indicating that the Mount Pagan caldera is very young and possibly historic in age. Locally includes stratigraphically lower and similar deposits on south caldera wall and northern sea cliff that may be related to earlier caldera collapses. Unconsolidated surface deposits in vicinity of Shomushon and south of the southern caldera rim may also include material from unit Qbp5 as well as unit Qbap15. Juvenile pumice includes both basalt with 2-5 percent plagioclase phenocrysts and aphyric basaltic andesite.

Qaf16

‘A‘ā flow underlying unit Qbap15 on north sea cliff. Basaltic andesite has about 1 percent plagioclase phenocrysts. Age, 235 ± 35 years B.P.

Qbf17

Three basaltic ‘a‘ā flows that underlie unit Qbap15 in old sea cliffs adjacent to the northeast coast of Mount Pagan. Top and middle flows have 7-10 percent plagioclase and less than 1 percent olivine phenocrysts. Lowest flow has 10-15 plagioclase and 7-10 percent olivine phenocrysts.

Qbf18

Two basaltic ‘a‘ā flows on the northeast flank of Mount Pagan that underlie unit Qbap15 in old sea cliffs 200-500 m near the coast. Upper flow has 25 percent plagioclase and less than 1 percent olivine phenocrysts. Lower flow has less than 1 percent plagioclase and olivine phenocrysts collectively.

Qbf19

Pāhoehoe and ‘a‘ā flows in large old sea cliff exposure near east-northeast coast of Mount Pagan. Unit underlies unit Qbap15 and overlies unit Qap20. Thickness is at least 40 m. Basalt has 1-2 percent plagioclase and less than 1 percent olivine phenocrysts.

Qap20

Surge deposits at the base of sea cliff on lower northeast flank of Mount Pagan. Fine-grained, well bedded, >20-m-thick deposit likely came from Mount Pagan, but its relationship to possible caldera-forming events is not known. Unit was not sampled for petrographic analysis.

Qbf21

Aerially extensive basaltic ‘a‘ā and pāhoehoe flows on the lower east and southeast flanks of Mount Pagan. Flows underlie Qbf3 and Qbf7, overlie the caldera rim, and are very late Holocene in age. Flow contains 30-40% plagioclase and <1% olivine phenocrysts.

Qbf22

‘A‘ā flow at coast on southeast flank of Mount Pagan. Underlies Qbf7. Basalt has 10-12 percent plagioclase and less than 1 percent olivine phenocrysts.

Qbc23

Surtseyan cone at coast on southeast flank of Mount Pagan. Cone was not sampled due to the lack of pristine material. All the tephra from this locality was either chemically or thermally oxidized.

Qbcf24

Spatter and cinder deposits of variable basaltic and silicic composition and an associated basaltic lava flow, on the Sengao Peninsula on the southeast flank of Mount Pagan. Basalt has less than 1 percent plagioclase phenocrysts. Tuffaceous silicic pumice is aphyric and appears to be the most silicic rock type of Pagan Island.

Qbcf25

Cinder deposits and an ‘a‘ā flow on the east side of the Sengao Peninsula. Basalt has 10-15 percent olivine phenocrysts and scattered xenoliths of gabbro.

Qv26

Inaccessible outer part of the Sengao Peninsula and adjacent small islands. Corwin and others (1957) show “undifferentiated lavas and pyroclastic rocks” in this area. Not sampled due to the fact that the rocks are altered and inaccessible.

Qbf27

Lava flow of apparent basaltic composition on south flank of Mount Pagan volcano 0.5 km south of southern caldera rim. Flow contains 15-20% plagioclase and 7-10% olivine phenocrysts. This flow is overlain by the volcanic breccia Qbap15.

Qbf28

Thick ponded ‘a‘ā flow on sea cliff on southwestern flank of Mount Pagan. Flow is about 10 m thick. Basalt has 3-5 percent olivine phenocrysts.

Qbf30

Three lava flows, mixed pāhoehoe and ‘a‘ā, on the southern caldera floor. Flow contains 25-35% plagioclase and <1% each of olivine and pyroxene phenocrysts. This unit is overlain by 1981 and Qbf7.

Qbf34

Pāhoehoe and ‘a‘ā flow of Bandeera Peninsula. Flow contains 5-7% each of plagioclase and pyroxene and 2-3% olivine phenocrysts.

Qbf35

Pāhoehoe flow along coast about 1 km north of Shomushon. Underlies unit Qbp5. Basalt has about 25-30 percent plagioclase and 1 percent olivine phenocrysts.

Qbf36

Pāhoehoe flow at coast 0.5 km west of Laguna Sanhiyon. Basalt has 6-12 percent plagioclase phenocrysts.

Qbf37

‘A‘ā flow at coast about 1 km northwest of Laguna Sanhiyon. Basalt has 5-10 percent plagioclase and 1-2 percent olivine phenocrysts.

Qbf38

‘A‘ā flow on north and east walls of inner eastern maar crater about 1 km northwest of summit of Mount Pagan. Basalt has 30-40 percent plagioclase, 5 percent olivine, and less than 1 percent pyroxene phenocrysts.

UNITS OF PLEISTOCENE AGE (restricted to lower south caldera wall)

Qaf29

‘A‘ā flows near the base of the southwestern caldera wall. Radiocarbon age of the second flow above the base is 10,780 ± 200 years B.P. (see map location). Interbedded with unmapped tuff, surge deposits, and pumice. Basaltic andesite is aphyric.

Qbf31

Twelve ‘a‘ā and pāhoehoe flows that form a prominent bluff near the center of the south caldera wall. Unit overlies Qbap32 and underlies the caldera-forming unit, Qbap15. One accessible flow has 30-40 percent plagioclase and 1-2 percent olivine phenocrysts.

Qbap32, Qbf32

Older tuff, surge, and pumice deposits on the southwestern caldera wall below unit Qaf29. Includes an interbedded ‘a‘ā flow (Qbf32). Eruption of this unit may have been associated with an earlier episode of caldera collapse. Rocks consist of basaltic andesite and basaltic pumice, blocks, and accidental xenoliths.

Qbf33

Two ‘a‘ā flows on the southeastern part of the caldera wall. Flows could be of Holocene age. Flow contains 12-15% plagioclase, 7-10% pyroxene and <1% olivine phenocrysts.

INTRUSIVE ROCKS

i

Intrusive rocks, generally dikes of basaltic composition. Commonly 1-2 m wide and dip a few degrees from vertical.

SURFICIAL DEPOSITS

Shown only where underlying volcanic rocks cannot be recognized. (also shown by Corwin and others, 1957).

Qal

Alluvium, consisting of clay- to boulder-sized fragments of volcanic rocks and minerals. Includes post-1981 debris flows that have destroyed and buried most of the village of Shomushon.

Talus

Talus, consisting of boulders and smaller rock fragments commonly at the bases of caldera walls (angular clasts) and sea cliffs (angular and rounded clasts).

Qb

Beaches, consisting of sand- to boulder-sized fragments of volcanic rocks and minerals and coralline limestone, possibly uplifted during magmatic inflation of Mount Pagan volcano.

Fill

Artificial fill, mainly loose dirt, under airplane runway. About half of the runway is buried by 1981 ‘a‘ā.

ACKNOWLEDGEMENTS

We thank the staff and Directors of the Emergency Management Office, Office of the Governor, Commonwealth of the Northern Mariana Islands, for considerable logistical support over the years. Meyer Rubin and Jack McGeehin dated the charcoal samples. John Sinton (University of Hawai’i-Manoa) analyzed rock samples. John Pallister and Steve Schilling contributed helpful reviews of the map and manuscript.

REFERENCES

Banks, N.G., Koyanagi, R.Y., Sinton, J.M., and Honma, K.T., 1984, The eruption of Mount Pagan volcano, Mariana Islands, 15 May 1981: Journal of Volcanology and Geothermal Research, v. 22, p. 225-269.

Corwin, Gilbert, Bonham, L.D., Terman, M.J., and Viele, G. W., 1957, Military geology of Pagan, Mariana Islands: U.S. Army Corps of Engineers, Intelligence Dossier, 259 p.

Hess, H.H., 1948, Major structural features of the western Pacific, an interpretation of H.O. 5485 Bathymetric Chart, Korea and New Guinea. Geological Society of America Bulletin, v. 59, p. 4 17-446.

Karig, D.E., 1971, Structural history of the Mariana Island Arc System: Geological Society of America Bulletin, v. 82, p. 323-344.

Karig, D.E., Anderson, R.N., and Bibee, L.D., Characteristics of back-arc spreading in the Mariana Trough: Journal of Geophysical Research, v. 83, p. 1213-1226.

Katsumata, M., and Sykes, L.R., 1969, Seismicity and tectonics of the Western Pacific-Isu-Mariana-Caroline and Ryukyu-Taiwan regions: Journal of Geophysical Research, v. 74, p. 5923-5948.

Kroenke, Loren, and 14 others, 1981, Initial Reports of the Deep Sea Drilling Project: U.S. Government Printing Office, Washington, D.C., v. 59, 276 p.

Le Bas, M.J., Le Maitre, R.W., Streckeisen, A., and Zanettin, B., 1986, A chemical classification of volcanic rocks based on the total alkali silica diagram: Journal of Petrology, v. 27, p. 745 750.

Moore, J.G., 2000, Density of basalt core from Hilo drill hole, Hawaii, Journal of Volcanology and Geothermal Research, v. 12, n. 1-4, p. 221-230.

Newhall, C.G., and Self, S., 1982, The volcanic explosivity index (VEI): An estimate of explosive magnitude for historical volcanism, Journal of Geophysical Research, v. 87, p. 1231-1238.

Newhall, C.G., and Dzurisin, D., 1988, Historical unrest at large calderas of the world: U.S. Geological Survey Bulletin 1855, 598 p.

Simkin, Tom, Tilling, R.I., Taggart, J.N., Jones, W.J., and Spall, Henry, 1989, This dynamic planet—World map of volcanoes, earthquakes, and plate tectonics: U.S. Geological Survey, scale 1:30,000,000.

Simkin, Tom, and Siebert, Lee, 1994, Volcanoes of the world: Geoscience Press, Inc., Tucson, 349 p.

Stern, R.J., and Bibee, L.D., 1984, Esmeralda Bank—Geochemistry of an active submarine volcano in the Mariana Island Arc: Contributions to Mineralogy and Petrology, v. 86, p. 159-169.

Tanakadate, Hidezo, 1940, Volcanoes in the Mariana Islands in the Japanese mandated South Seas: Bulletin Volcanologique, v. 18, p. 199-225.

Trusdell, F.A., Moore, R.B., Sako, M, White, R.A., Koyanagi, S.K., Chong, R. and Camacho, JT., 2005, The 2003 eruption of Anatahan volcano, Commonwealth of the Northern Mariana Islands: Chronology, volcano logy, and deformation, Journal of Volcanology and Geothermal Research, v. 146, p.184-207

Appendix A: Recalculation of tephra deposits based on Banks et al isopach data.

We calculate the on-land volume‡ of tephra to be:*

12.7 million m^3

*(*For this calculation we use the isopach contours and reported in Banks and others,* 1984 and the cut and fill functions in ArcGIS) Banks reports an on-*land estimate of tephra to be* about 28 x 10^6 m^3 or about 11 x 10^6 m^3 of magma (page 15).

Using an average density of basalt = 2.55g/$cm^{3\dagger}$ *(as reported by **Moore, 2000** Density of basalt core from Hilo drill hole, Hawaii. JVGR vol112 n.1-4 p.221-230).*

†*The 1981 deposits are basalt.*

Therefore 1 cubic meter of basalt = 2.55 g/cm x 100 cm x 100 cm x 100 cm g/m^3 = 2.55 million grams/m^{3*} or 1 cubic meter of basalt = 2.55 Mt

**1 metric ton = 1000kg = 1 million grams = Mt*

To get Metric tons (Mount):

Based on our estimate*‡ = 12.7 million m^3 x 2.55 Mt/m^3 = **32.4 million Mt**

Based on Bank's estimate = 28 million m^3 x 2.55 Mt/m^3 = **71.4 million Mt**

Calculation of volume of tephra on Pagan according to Azmar:

Weight of tephra on Pagan according to Azmar: 200 million Mt

Therefore volume converted back to millions of cubic meters on the ground 200 million Mt / 2.89 (density used by Azmar) = **69.2 million m^3**

‡*-Our volume calculations do not account for the amount of erosion that has occurred in the 24 years since the eruption and the porosity of the pozzolan.*

Volume of 1981 tephra on Pagan

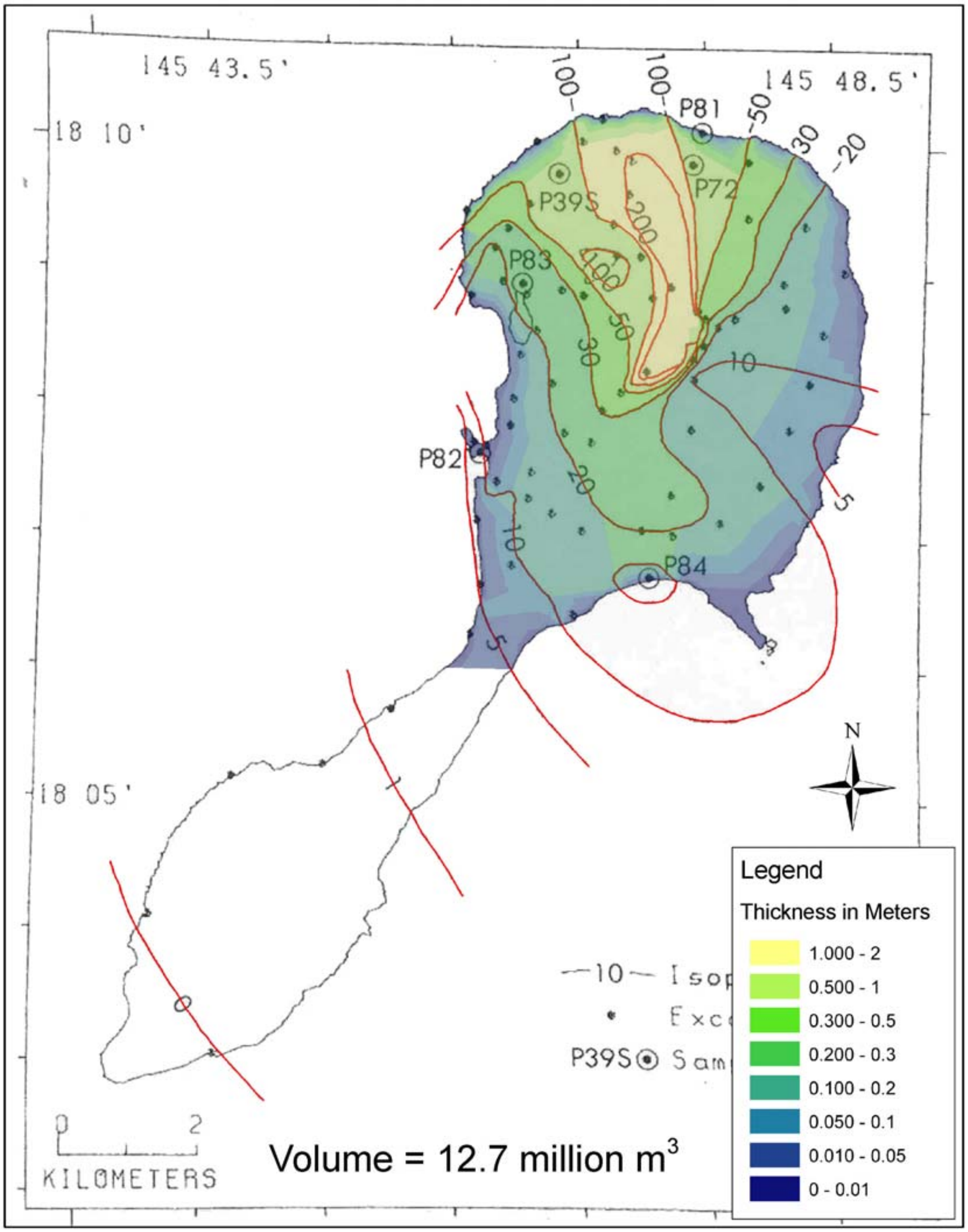

Figure 1. Colored area represents the region included in our volume calculation. The lines represent tephra thickness in centimeters.

Appendix B

An Investigation of

VOLCANIC EJECTA FROM THE SAIPAN ERUPTION

prepared for

USGS Volcano Hazards Program

Project 11271-001 - MI 5022-MAR06
April 5, 2006

NOTE:
This report refers to the samples as received.

Introduction

One sample of volcanic rubble labelled SAIPAN was submitted for mineralogical characterization by Dr. J. Quick on behalf of the USGS Volcano Hazards Program. In addition to fundamental characterization, the suitability of this material as a pozzolan is being investigated. Pozzolans are materials, usually glassy, which react with calcium-hydroxide to form compounds with cementitious properties. Although the most commonly used pozzolan is fly-ash, a natural source is desirable.

Chris Hamilton, M.Sc.
Consulting Mineralogist

Joe Zhou, M.Sc., P.Geo.
Group Leader, Process Mineralogy

Experimental work by: K. Henderson, N. Morton & C. Hamilton
Report preparation by: C. Hamilton

Report Summary

Sample and Scope

One 2.3 kilogram sample of volcanic rubble or ejecta from the Saipan Volcanic eruption of April 2005, in the North Marianas Islands was received for mineralogical investigation.

Methods Used

The sample was photographed in as-received form and subsequently split into two roughly equivalent sub-samples using a rotary splitter. One half was kept as spare and the other half stage-crushed to 100% passing 850 micrometers or 20 mesh. One polished thin section and two polished sections were prepared of a representative 200 gram portion of the passing 850 micrometer material for optical and scanning electron microscopic (SEM) analysis. The remainder of the 200 gram, passing 850 micrometer sub-sample was also kept as spare, while the balance of the passing 850 micrometer sample-half was pulverized for X-Ray Diffraction analysis and a chemical assay. Certified assays are presented in Appendix C.

Optical microscopy was performed in both transmitted and reflected light and, as the sample was composed of volcanic glasses ranging from clear to opaque, the technique elected to perform modal analysis was QEMSCAN, an acronym for **Q**uantitative **E**valuation of **M**aterials by **Scan**ning Electron Microscopy. It is a SEM-based technique in which materials are identified and quantified by a combination of back-scattered electron (BSE) signal intensity and Energy Dispersive X-ray Spectroscopy (EDS). The SGS Lakefield system used was a Leo 440 SEM with light-element equipped EDS using standard operating conditions as follows:

Accelerating Voltage = 25 kV

Beam Current = 3 nA

A Bulk modal analysis was performed in linear intercept analysis mode

A "Mini-Particle Map" Analysis to elucidate particle variability based on chemical and textural attributes.

Results – Petrography

A photomicrograph of the as-received sample is presented in Figure 1, from which it is evident that particles range in size from one inch (2.5 centimeters) down to dust-sized material. The median as-received particle size was between 0.5 and 1 centimeter. Particles are highly porous (Figure 2) and generally rusty, drab olive-grey in colour. Some nearly black, obsidian-like particles are present, as well as traces of creamy white fragments finer than 5 millimeters in size.

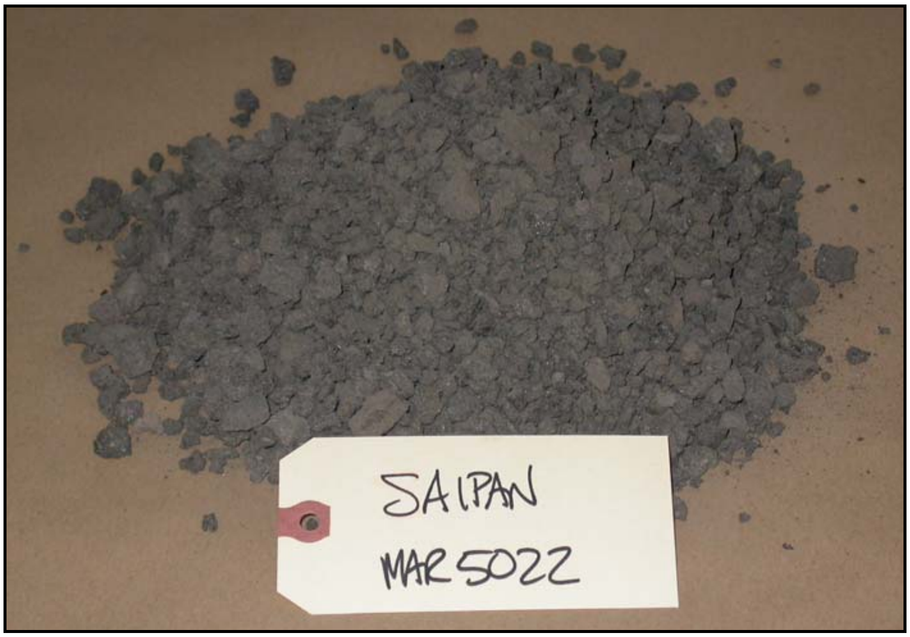

Figure 1. Digital photograph of a representative portion of the as-received sample. The sample label is 12 centimeters long and 6 centimeters wide. For reference, the background is brown glossy kraft paper.

Figure 2. Digital photograph of a selection of coarse fragments showing a high degree of porosity.

In thin section, the range of microtextures evinced by the material is significant. Figures 3 through 6 show typical textures of resulting particles after crushing to passing 850 micrometers.

(In this respect, it is important to note that the high porosity makes this material extremely easy to crush.)

Glassy particles totally barren of crystalline materials are comparatively rare, even after grinding. Crystalline products range from very fine-grained, quenched microcrystallites of feldspar, pyroxene and Fe-oxides through to microphenocrysts and phenocrysts of feldspar, pyroxene and olivine. Quenched microcrystallites range between 5 and 30 micrometers in size, while microphenocrysts range from 150 to 800 micrometers in size. Phenocrysts are dominated by feldspar and are seldom larger than 1 millimeter in size. Large white particles present in the sample up to 2 mm in size are typically calcite.

The range in textures are largely a result of relative rates of cooling, though magnetite-rich particles are clearly a consequence of more iron rich melt compositions, and probably more advanced crystallization prior to eruption. Olive green to brown, clear glasses are directly quenched from the molten state and possess variable microlites of feldspar formed prior to quenching, while skeletal overgrowths on feldspars clearly occurred during or immediately prior to eruption.

Although some authors refer to many feathery textures in volcanic glasses as devitrification products, textures ascribed to devitrification were not observed in the studied sample. (Devitrification, or reverting from the glassy to crystalline state, usually takes place over a lengthy geological time-frame of the order of millions of years.)

In general, glassy particles contain at least 90% glass, while more opaque particles are substantially less glassy but the glass content seldom falls below 50%. As a result, although opaque particles will be less amenable to react as a pozzolan than glassy particles, the ratio of opaque to glassy particles is not likely to materially affect overall reactivity.

Rare, large angular Fe-oxide particles up to 1 mm in size were observed in the sample. These particles are represented by goethite and associated Fe-oxyhydroxides and do not appear to be par t of the volcanic assemblage. Fe-oxides in the eruptive phase appear to be almost exclusively magnetite with minor accompanying hematite as fine platelets within- or attached to – magnetite.

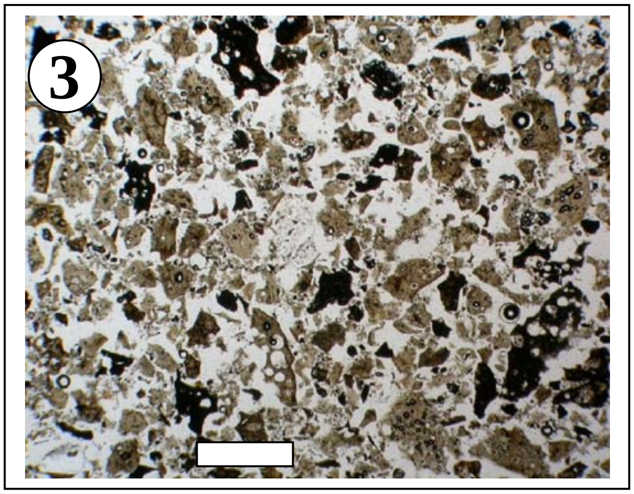

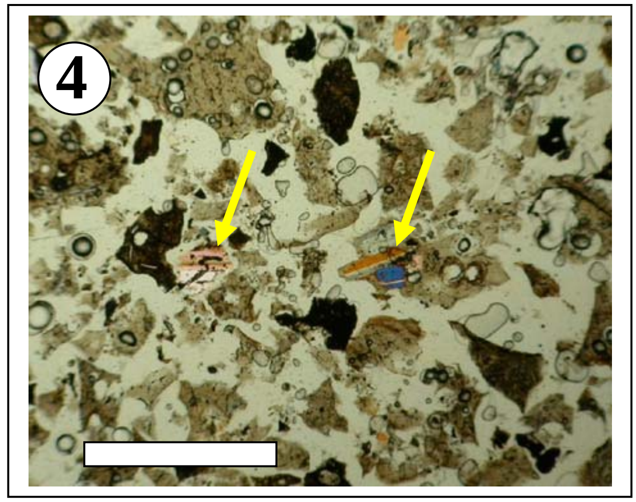

Figure 3. Transmitted light photomicrograph of the submitted sample crushed to passing 850 micrometers. The white grain in the centre of the field of view (arrowed) is a feldspar crystal. Scale bar is 1 mm.

Figure 4. Higher magnification view of glassy shards under partially polarized light, showing feldspar crystals (slightly thick in section) in shades of blue and orange (yellow arrows). Olive green, glassy shards outnumber opaque shards in an approximate 5:1 ratio. Scale bar is 1 mm.

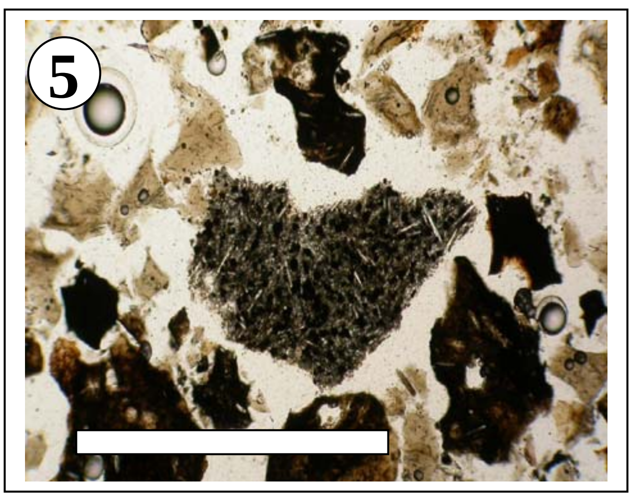

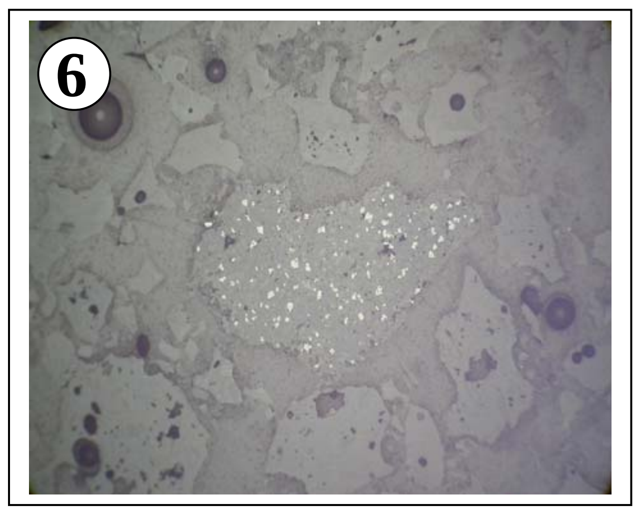

Figure 5. A selection of opaque to semi-opaque particles, most of which are brown in colour and glassy. The central particle, by contrast, is lighter grey and has felt-like texture of quenched plagioclase. Transmitted light. Scale bar is 1 mm.

Figure 6. Reflected light image of the same view in figure 5, showing abundant magnetite crystals associated with interstitial glass between plagioclase. Scale bar is 1 mm.

Results – XRD Analysis

X-ray diffraction analysis (Appendix C) reveals that the material is largely amorphous, with positively identified crystalline species including plagioclase feldspar predominantly, minor olivine and pyroxene and a trace amount of calcite. Three tentative identifications based on single-peak matches suggest the possible presence of a smectite clay (peak at 12.1 Ångstroms), a possible zeolite-like mineral (peak at 11.4 Ångstroms) and an amphibole ((peak at 8.3 Ångstroms). Whereas the latter might represent a primary phase which crystallized along with olivine and plagioclase (i.e. pre-eruptive), the former would reflect possible derivation by alteration of the glassy phase post eruption, and is consistent with natural reactivity of the glass.

Results – SEM Analysis

A point-counting method was performed whereby the relative proportions of glass and crystalline material was estimated on a per-particle basis and the frequency of particles in each category determined. Results are presented in Table 1, from which it is evident that the median particle contains between 60 and 80% glass, or 68.2% glass, after crushing to passing 850 micrometers particle size. A weighted distribution was calculated but requires an accurate determination of the specific gravity of the glassy phase to be accurate. Modal analyses are presented in Table 3.

% Glass in particle	% Volume of material	Est. % by weight
>80	3.3	4.3
60-80	79.4	84.0
40-60	12.6	10.1
20-40	3.3	1.5
0-20	1.4	0.1
0	0.3	<0.1
All material	100.0	100.0

Table 1. Approximate distribution of material reporting to volumetric categories of glassy phase. (Est. is an abbreviation for estimated. See text for details.)

The grain size distributions of the primary crystalline species was determined by automated linear intercept analysis across the polished section, with a pixel-to-pixel point spacing of 2.7 micrometers. Results are tabulated overleaf and graphically portrayed in Figure 7.

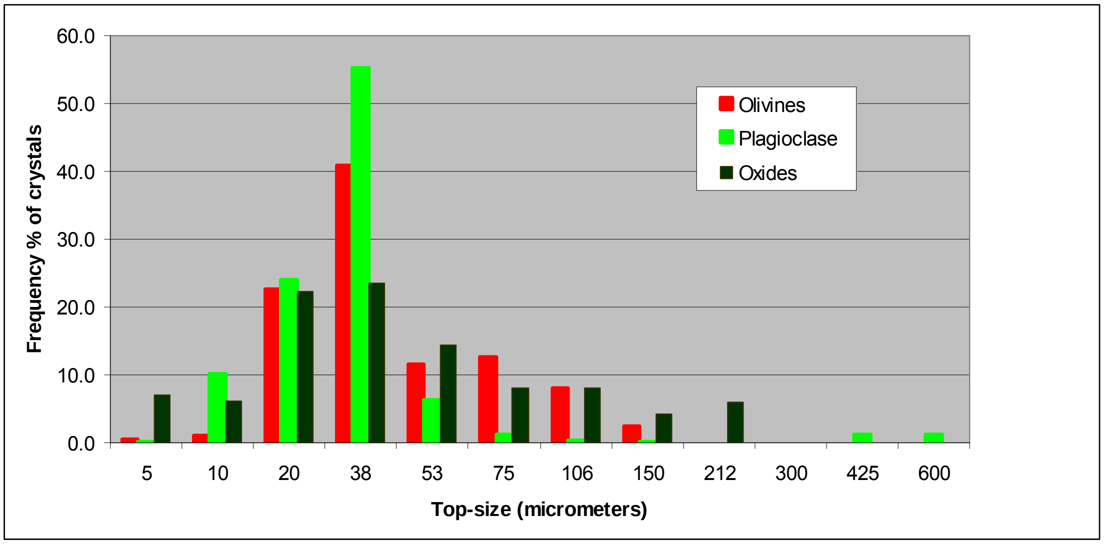

Top size	5	10	20	38	53	75	106	150	212	300	425	600	850
Olivine	0.5	1.1	22.6	40.9	11.7	12.7	8.1	2.5	0.0	0.0	0.0	0.0	0
Plagioclase	0.2	10.1	24.0	55.2	6.4	1.2	0.4	0.2	0.0	0.0	1.1	1.2	0
Oxides	7.0	6.2	22.3	23.6	14.5	8.1	8.0	4.3	6.0	0.0	0.0	0.0	0

Table 2 & Figure 7. Grain size distributions based on linear intercept data by automated analysis. (Based on 870,000 individual intercepts)

Mineral/Phase	%
Glass	65.9
Plagioclase	31.2
Clinopyroxene	1.4
Olivine	1.2
Oxides	0.2
Carbonates	<0.05
Quartz	<0.05

Table 3. Modal analysis as determined by linear intercept analysis.

Conclusions

- A whole-rock and mineralogical analyses has been presented for a representative portion of the submitted sample crushed to passing 850 micrometers.
- The material is composed of approximately 66% glass, and is considered a suitable candidate as pozzolan. Most crystalline material within the glassy matrix should be inert and not pose any problems to utilization as such
- Liberated crystalline materials include feldspar phenocrysts which will be inert, carbonates which may assist in pozzolanic reactions, and oxides which may be amenable to removal by magnetic or gravity separation if desirable.
- Confirmation of the presence of swelling clay is recommended to rule out the likelihood of deleterious properties these may introduce.
- No sulphur is present which is advantageous.

APPENDIX C:

Certified Chemical Assay results

SGS
SGS Lakefield Research Limited
P.O. Box 4300 - 185 Concession St.
Lakefield - Ontario - KOL 2HO
Phone: 705-652-2038 FAX: 705-652-6441

LR Internal Dept 14
Attn : CH/Anita C

---, ---

Phone: ---
Fax:---

Tuesday, April 04, 2006

Date Rec. : 29 March 2006
LR Report : **CA00555-MAR06**
Project : CALR-11271-001
Client Ref : MI5022-MAR06

CERTIFICATE OF ANALYSIS

Final Report

Sample ID	SiO2 %	Al2O3 %	Fe2O3 %	MgO %	CaO %	Na2O %	K2O %	TiO2 %	P2O5 %	MnO %	Cr2O3 %	V2O5 %	LOI %	Sum %	S %	S= %	SO4 %	S° %
1: Saipan (850um)	50.8	15.8	12.5	5.09	10.3	2.56	0.76	0.89	0.14	0.21	0.02	0.07	-0.20	98.9	0.01	< 0.01	< 0.4	< 0.5

Debbie Waldon
Project Coordinator,
Minerals Services, Analytical